International Journal of Modern Manufacturing Technologies
ISSN 2067–3604, Vol. XV, No. 2 / 2023
https://doi.org/ 10.54684/ijmmt.2023.15.2.20

OPTIMIZATION OF CUT QUALITY FOR AWJ PROCESSING OF A STEEL ALLOY

Bogdan Chirita, Eugen Herghelegiu, Crina Radu, Cosmin Grigoras, Catalin Tampu

"Vasile Alecsandri" University of Bacau-Romania, Department of Industrial Systems Engineering and Management, Calea Moldovei, No. 157, 600115, Bacau, Romania

Corresponding author: Bogdan Chirita, chib@ub.ro

Abstract: Abrasive water jet (AWJ) has gained an important place among the machining technologies due to its capacity to cut complex shapes in various materials without thermal effects and with low cutting forces, but it also has a reduced environmental impact. A key element for the quality of the cut is the amount of energy contained in the abrasive jet. The dissipaton of energy leads to kerf taper, high values of surface roughness, surface striations, the deviation of the water jet (jet drag), and even insufficient penetration. The current paper investigates the influence of process parameters on the quality of the cut for a S235 steel alloy. The quality of the cut was assessed by four parameters: entrance width of cut (Li), exit width of cut (Le), perpendicularity (u) and kerf angle (α). The experiments were organized according to a D-optimal Response Surface Method. Analysis of variance (ANOVA) was used for the development of a mathematical model that correlates the influence of process parameters on the quality of the cut. Finally, an optimization of the process parameters was proposed.
Key words: Abrasive Water Jet (AWJ), S235 steel alloy, cut quality, ANOVA.

1. INTRODUCTION

Abrasive water jet (AWJ) is an alternative machining process that has gained lately an increased importance for the industrial applications. The working principle is based on the eroding force that a combination of high-pressure water jet and abrasive particles exerts on the processed material. The versatility of AWJ comes from the capacity to cut intricate contoured shapes, a large range of materials from ductile to brittle, with low cutting forces and no heat affected zone. AWJ is also considered an environmentally friendly process because all the byproducts can be recycled.

However, there are numerous factors to be taken into consideration during machining, such as water jet pressure, flow rate of the abrasive material, abrasive material type, traverse speed, the standoff distance, the water jet impact angle, and others that impact the surface quality, the geometry of the cut or the material removal rate. A key element for the quality of the cut is the amount of energy possessed by the abrasive jet. The dissipation of energy leads to kerf taper, increased surface roughness, surface striations, the deviation of the water jet (jet drag), and even insufficient penetration.

Babu and Muthukrishnan [1] investigated the effect of process parameters (feed rate, water pressure, standoff distance, and abrasive flow rate) on the surface roughness and kerf-angle of AISI 1018 mild steel. The experiments were organised according to a Taguchi L27 orthogonal array, and response surface method (RSM) was applied in the optimization phase. RSM was also used by Deshpande et al [2] for surface roughness and cone angle optimization in AWJ machining of Inconel 718 alloy based on three input factors (the travel speed, abrasive flow rate and standoff distance). Desirability analysis was applied by Vijayakumar et al. [3] to determine the ideal values of process parameters to generate quality holes on Inconel-625 space alloy by abrasive water jet hole-making. Sisodia et al. [4] studied the impact of jet-water pressure, nozzle traverse rate, and stand-off height on surface roughness and kerf taper properties of hardened AISI 440C stainless steel using RSM for experimental planning and process optimization. An experimental study by Wang et al [5] approached the influence of processing parameters (cutting speed, water pressure, abrasive flow rate, material thickness) on deviation error of the kerf profile. Du et al [6] have studied the internal mechanism of the AWJ cutting of DH-40 high-strength steel. RSM was applied to design parameter analysis experiments and for optimization. Another test was carried to regress the dissipated power function of the waterjet and a simplified mathematical model of the cutting front profile was established. Abushanab et al [7] employed statistical and physical analysis to study the parameters influence of AWJ machining on Ti6Al4V alloy. Water pressure, abrasive flow rate, feed rate and stand-off distance were used to investigate the influence on the post-processing surface characteristics. Llanto et al [8]

investigated the impact of traverse speed and material thickness on kerf geometries and material removal rates for contour cutting of AISI 304L. Joel and Jeyapoovan [9] studied the machinability of AA7075 aluminium alloy using Taguchi method and Grey relational analysis was applied for multi-parameter optimization. Radovanovic [10] used multi-objective genetic algorithm for simultaneous optimization of productivity and operating cost of the AWJ cutting of S235 carbon steel. Ćojbašić et al [11] proposed extreme learning machine method for the estimation of surface roughness obtained from AWJ cutting of AA-6060 aluminium alloy and compared the results with the predictions from genetic algorithms and artificial neural networks methods.
The current paper investigates AWJ cutting of S235 steel alloy from the perspective of the influence of process parameters on the quality of the cut, which was assessed by four parameters: entrance width of cut (Li), exit width of cut (Le), perpendicularity (u) and kerf angle (α). The experiments were organized according to a D-optimal Response Surface Method.

2. MATERIALS AND METHODS

The experiments were performed on 19 mm thick plates made of S235 steel alloy, a material widely used for metal structures. Table 1 presents the chemical composition of the material, while Table 2 shows data on the mechanical properties.

Table 1. S235 steel chemical composition

Elements	C	Si	Mn	P	S	N	Cu	Cr	Ni	Mo	Al	V
Weight %	0.13	0.25	0.58	0.013	0.008	0.01	0.32	0.08	0.10	0.013	0.033	0.001

Table 2. S235 mechanical strength

Yield strength MPa	Ultimate strength MPa	Elongation %	Impact resistance KV J	Brinell hadness HB
235	360 - 510	25	27	100 - 154

Machining was executed on OMAX MAXIEM 0707 JetMachining Center with the following technical specifications: X-Y Cutting travel 794×775 mm, Z-axis travel 305 mm, table size 1435×953 mm, maximum jet pressure 3500 bar, accuracy ±0.076 mm, repeatability ±0.025 mm (Figure 1a) [12]. The focusing tube had the length L_f = 102 mm and the diameter D_f = 0.74 mm. The abrasive material was garnet with a granulation of #80. According to the specifications of ISO/WD/TC 44 N 1770 standard, the quality of the cut was estimated by four dimensional parameters: entrance width of cut (Li), exit width of cut (Le), perpendicularity (u) and kerf angle (α) (Figure 2). The measurements were carried with a profile projector Mitutoyo PH-A14 (Figure 1b).

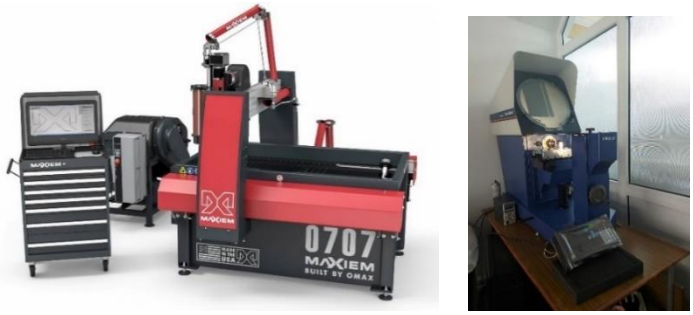

(a) (b)

Fig. 1. Experimental equipment: (a) AWJ cutting machine [12]; (b) Profile projector

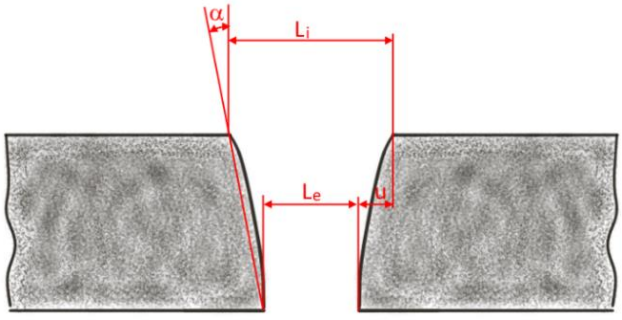

Fig. 2. Kerf profile parameters

The design of experiments was organized with Design-Expert software, according to a D-optimal Response Surface Method using three input factors: cutting quality (Q), the cutting pressure (p), and the standoff distance (h). As the objective of this study was to develop a technology usable in the industrial environment, the first input factor, cutting quality, was chosen as it was implemented in the machine control parameters, according to the producer specifications. Cutting quality (Q) has five levels, Q1 to Q5, where Q1 corresponds to faster traverse speed and the lowest quality, while Q5 uses lower speed to generate a superior cut quality. The second input factor was the cutting pressure (p) for which three values (variation levels) were chosen, 200 MPa, 250 MPa, and 300 MPa respectively. The standoff distance (h), which measures the distance between the nozzle and the part, is the third input factor, also with three levels of 1 mm, 2 mm and 3 mm. The combination led to a 45 runs design of experiments. Analysis of Variance (ANOVA) was used to show the effects of the factors on the responses and to establish the significant factors using a stepwise elimination algorithm that generates the best fitted model.
The prediction capability of the models is estimated using a series of correlation coefficients (R^2, Adj.R^2, Pred.R^2). R^2 measures the amount of reduction in data variability, with values within [0,1] interval, and is calculated as a ratio between the sum of squares of the model and the total sum of squares (Equation 1). Because R^2 increases as more terms are added to the model, even though the precision is not always higher, an adjusted coefficient (Adj.R^2) is preferred as it includes only the statistically significant terms (Equation 2) [13].

$$R^2 = \frac{SS_{Model}}{SS_{Total}} \tag{1}$$

$$Adj.R^2 = \frac{SS_{Model} / (n-p)}{SS_{Total} / n-1} \tag{2}$$

The prediction capability (Pred.R^2) of the regresion model is calculated using the following equation:

$$Pred.R^2 = 1 - \frac{PRESS}{SS_{Residual} + SS_{Model}} \tag{3}$$

where *PRESS* is the predicted residual error sum of squares that measures how the model fits each point in the design, SS_{Model} – model sum of squares, SS_{Total} – total sum of squares, $SS_{Residual}$ – residual sum of squares, n – the number of observations (experiments), p – number of model parameters. A difference of less than 0.2 between Adj.R^2 and Pred.R^2 is recommended.

3. RESULTS AND DISCUSSION

3.1 Analysis of variance

The results of ANOVA are presented in Table 3. One can see that the models contain linear terms, interactions and square terms as the source of variability. A term is considered significant if the corresponding p-value is smaller than 0.05. Occasionally, models may include non-significant terms (p-value>0.05) if they are involved in significant interactions, to preserve the hierarchy.
ANOVA for entrance width of cut Li shows a quadratic model for which the standoff distance h has the highest contribution (60.40%) followed by the cutting quality Q (33.93%) and to a much-limited extent by the quadratic form of the standoff distance (0.63%). There is a very good agreement between Adj. R^2 and Pred. R^2 and the model can predict 92.88% of the response variation. The influence of the two factors is presented in Figure 3. a larger entrance width of the cut Li results from the increase of the standoff distance because the jet is spreading as it leaves the focusing tube. a wider cut results for Q5 due to the lower traverse speed that allows the abrasive jet to act for increased amounts of time. When the cutting quality parameter shifts toward Q1, the traverse speed increases, therefore the abrasive jet interacts with the material for smaller time periods and the width of the cut is smaller.

Table 3. ANOVA results

Source	DF	Sum of squares	Mean square	F-value	p-value	% Contribution
Entrance width of cut, Li						
Model	6	0.3145	0.0524	118.43	< 0.0001	
A: cutting quality, Q	4	0.1124	0.0281	63.47	< 0.0001	33.93
C: standoff distance, h	1	0.2001	0.2001	452.09	< 0.0001	60.40

C^2		1	0.0021	0.0021	4.64	0.0376	0.63
Residual		38	0.0168	0.0004			
Total		44	0.3313				
R^2	0.9492		Adj. R^2	0.9412	Pred. R^2	0.9288	
Exit width of cut, Le							
Model		7	0.7252	0.1036	240.02	< 0.0001	
A: cutting quality, Q		4	0.6876	0.1719	398.24	< 0.0001	92.82
B: pressure, p		1	0.0000	0.0000	0.0692	0.7940	-
C: standoff distance, h		1	0.0501	0.0501	116.06	< 0.0001	6.76
B×C		1	0.0031	0.0031	7.14	0.0113	0.42
Residual		36	0.0155	0.0004			
Total		43	0.7408				
R^2	0.9790		Adj. R^2	0.9749	Pred. R^2	0.9685	
Perpendicularity, u							
Model		7	0.0776	0.0111	105.38	< 0.0001	
A: cutting quality, Q		4	0.0639	0.0160	151.78	< 0.0001	78.50
B: pressure, p		1	0.0001	0.0001	0.9739	0.3303	-
C: standoff distance, h		1	0.0115	0.0115	109.05	< 0.0001	14.13
B×C		1	0.0004	0.0004	3.37	0.0748	0.49
Residual		36	0.0038	0.0001			
Total		43	0.0814				
R^2	0.9535		Adj. R^2	0.9444	Pred. R^2	0.9318	
Kerf angle, α							
Model		7	0.7057	0.1008	105.41	< 0.0001	
A: cutting quality, Q		4	0.5808	0.1452	151.80	< 0.0001	78.47
B: pressure, p		1	0.0009	0.0009	0.9718	0.3308	-
C: standoff distance, h		1	0.1043	0.1043	109.09	< 0.0001	14.09
B×C		1	0.0032	0.0032	3.36	0.0750	0.43
Residual		36	0.0344	0.0010			
Total		43	0.7402				
R^2	0.9535		Adj. R^2	0.9444	Pred. R^2	0.9318	

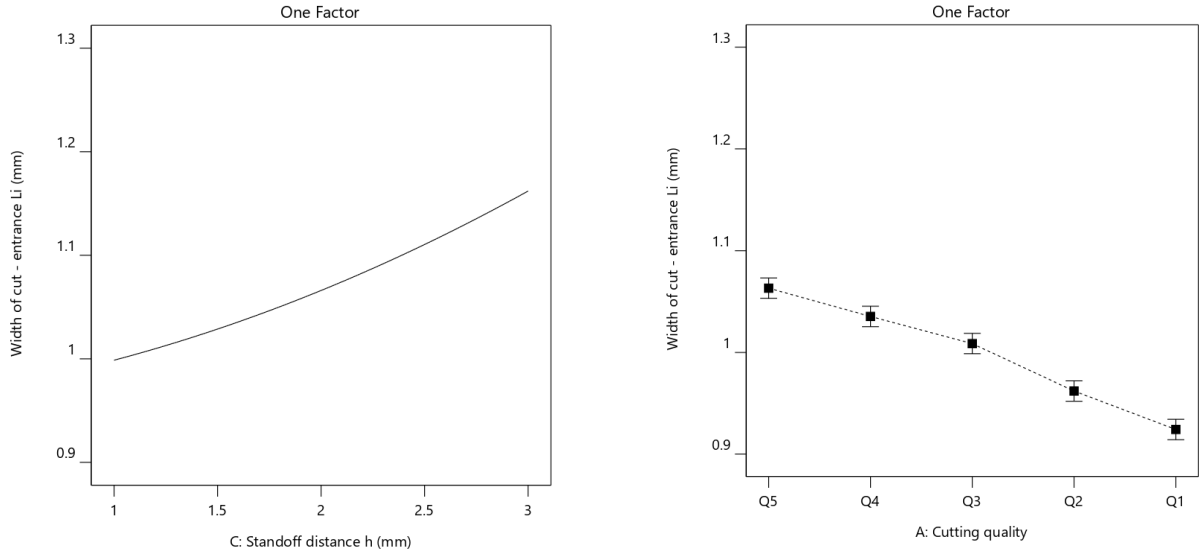

Fig. 3. Influence of standoff distance h and cutting quality Q on entrance width of cut Li

The second analysis has the exit width of cut Le as response. The best fitted model is a two-factor interaction for which the significant factors are: the cutting quality Q, with 92.82% contribution, standoff distance h, with 6.76% contribution, and the interaction pressure - standoff distance, with a very small contribution of only 0.42%. The Adj.R2 and Pred.R2 are in good agreement and the model may explain almost 97% of the response variability. In a similar maner with the anterior response, a wider exit width of cut results for Q5 cutting quality parameter because of the lower traverse speed that increases the action time for the AWJ. Due to the increased traverse speed

from Q1, the exit width of cut Le decreases to minimum. When the standoff distance increases from 1 mm to 3 mm leading to a larger distance between the cutting head and the surface of the part, the water jet spreads wider, causing the extension of the width of cut. The interaction between the water jet pressure and the width of cut (B×C) is also statistically significant, although to a lesser extent. The influence of the pressure is especially pregnant for the lower value of the standoff distance (1 mm) where it leads to a slight extension of the width of cut. Higher AWJ pressure signifies a higher cinematic energy of the abrasive particles thus capable to remove more material, therefore a wider cut. The increase of the standoff distance diminishes the efficiency of the interaction. Figure 4 shows the influence of the input factors on exit width of cut.

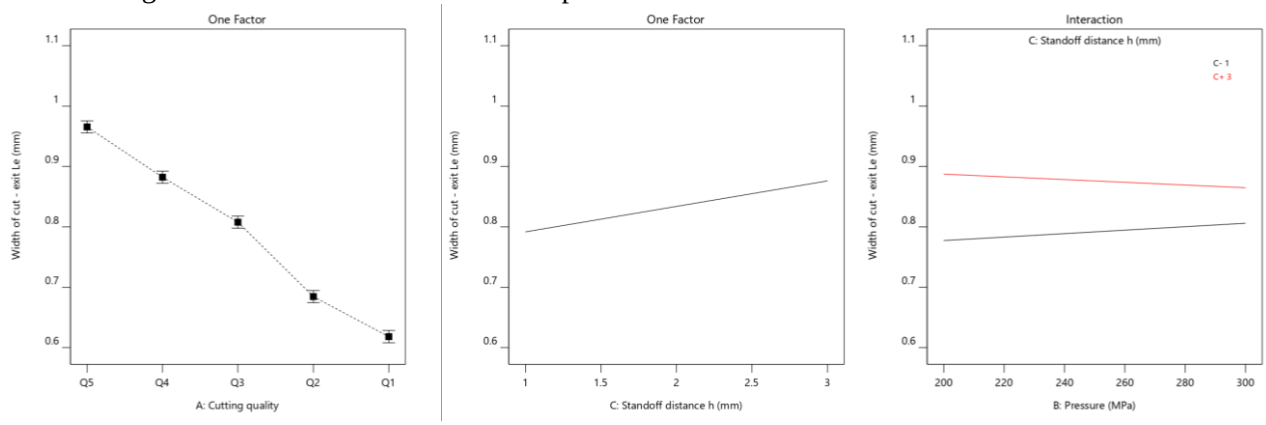

Fig. 4. Influence of cutting quality Q, standoff distance h and the interacton pressure – standoff distance on exit width of cut Le

The ANOVA for perpendicularity u has also shown that the best fitted model is a two-factor interaction for which the statistically significant factors are the cutting quality Q with 78.5% contribution, followed by the standoff distance h, with 14.13% contribution, and finally by the interaction pressure-standoff distance with a contribution of 0.49%. The model is fit, with a very good agreement between Adj.R2 and Pred.R2 and it can predict more than 93% of the response variability. The influence of the factors on perpendicularity is presented in Figure 5. The smallest value of perpendicularity u (corresponding to a wall that is closest to the vertical) is obtained for Q5 cutting quality. This is because in this case the traverse speed is the lowest, which gives the AWJ the possibility to perform an almost straight cut with small differences between the entrance and the exit width of cut. When the cutting quality shifts toward Q1, the deviation from the perpendicular position of the wall increases. The efficiency of the water jet is reduced by the increase of the standoff distance and the perpendicularity has a rising trend. The interaction pressure – standoff distance shows that the increase of pressure restrains the influence of the standoff distance.

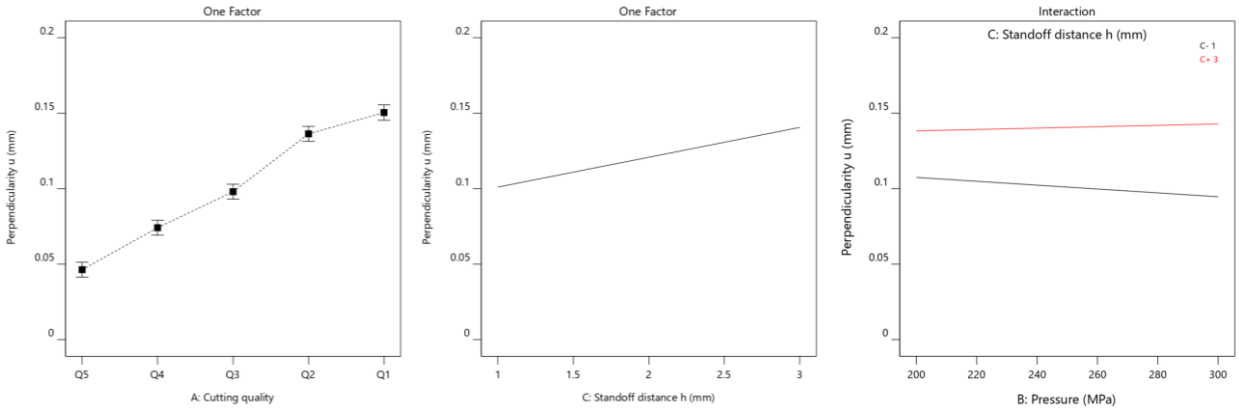

Fig. 5. Influence of cutting quality Q, standoff distance h and the interacton pressure – standoff distance on perpendicularity u

The last response taken into consideration was the kerf angle α. The ANOVA for this response has yielded very similar results with the perpendicularity u, as these two are closely related. The statistically significant factors are the cutting quality Q with 78.47% contribution, followed by the standoff distance h, with 14.09% contribution, and finally by the interaction pressure-standoff distance with a contribution of 0.43%. The model is fit, with a very good agreement between Adj.R2 and Pred.R2 and it can predict more than 93% of the response variability. The influence of the factors on perpendicularity is presented in Figure 6.

3.2. Mathematical models

Besides finding the significant factors, RSM is used to determine mathematical models of the output. Second order polinomial equations (Equation 4) are used to link the input factors and the responses, the equation coefficients being determined by regression using the least square method.

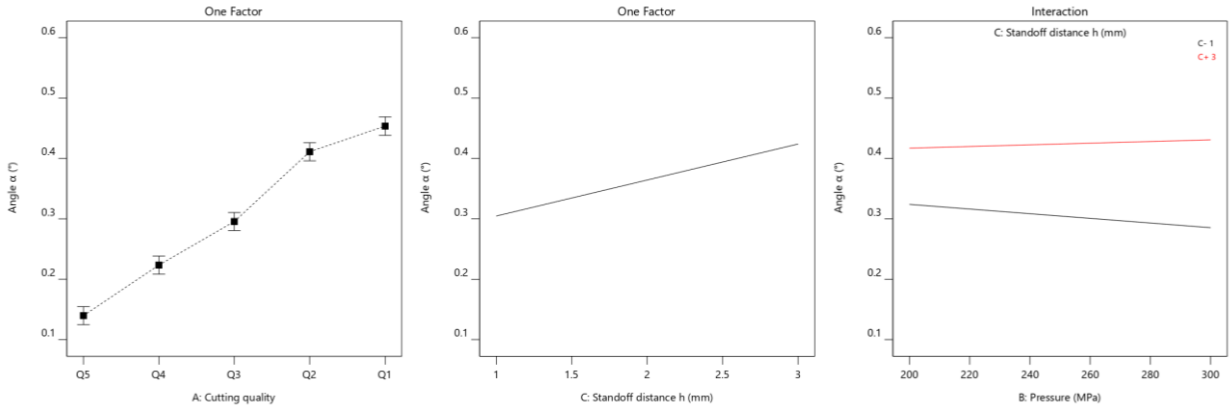

Fig. 6. Influence of cutting quality Q, standoff distance h and the interacton pressure-standoff distance on kerf angle α

$$y = \beta_0 + \sum_i \beta_i x_i + \sum_i \beta_{ii} x_i^2 + \sum_i \sum_{j>i} \beta_{ij} x_i \times x_j + \varepsilon \quad (4)$$

where x_i are the input factors, α_0 is the free term, α_i are the linear term coefficients, α_{ii} are the quadratic term coefficients, α_{ij} are the interaction coefficients, and ε is the error.

Due to the fact that cutting quality is a calitative factor (non-numeric) an equation was generated for each of the five levels.

For the the entrance width of cut Li, the equation coefficients are presented in Table 4. The values predicted by the model follow the actual data quite accurately, as can be seen in Figure 7.

$$Li_k\,(h) = \beta_{0k} + \beta_{1k}\,h + \beta_{11k}\,h^2 \quad (5)$$

where k = 1…5, corresponding the coefficients of Qk.

Table 4. Equation coefficients for the entrance width of cut Li model

Coefficients	Q1	Q2	Q3	Q4	Q5
α_0	+0.885556	+0.923333	+0.970000	+0.996667	+1.02444
α_1 (h)	+0.024333	+0.024333	+0.024333	+0.024333	+0.024333
α_{11} (h^2)	+0.014333	+0.014333	+0.014333	+0.014333	+0.014333

For the the exit width of cut Le, the equation coefficients are presented in Table 5. The values predicted by the model closely follow the actual data, as can be seen in Figure 8.

For the the perpendicularity u, the equation coefficients are presented in Table 6. The values predicted by the model closely follow the actual data, as can be seen in Figure 9.

The model for the the exit width of cut Le is given in Equation 6, with the coefficients presented in Table 5. The values predicted by the model closely follow the actual data, as can be seen in Figure 8.

$$Le_k(h, p) = \beta_{0k} + \beta_{1k}p + \beta_{2k}h + \beta_{12k}p \times h \quad (6)$$

where *k = 1…5*.

The values predicted by the model closely follow the actual data, as can be seen in Figure 9.

$$u_k(h, p) = \beta_{0k} + \beta_{1k}p + \beta_{2k}h + \beta_{12k}p \times h \quad (7)$$

where *k = 1…5*.

Table 5. Equation coefficients for the exit width of cut Le model

Coefficients	Q1	Q2	Q3	Q4	Q5
α_0	+0.440281	+0.506516	+0.629849	+0.704293	+0.787627
α_1 (p)	+0.000543	+0.000543	+0.000543	+0.000543	+0.000543
α_2 (h)	+0.106233	+0.106233	+0.106233	+0.106233	+0.106233
α_{12} (p×h)	-0.000256	-0.000256	-0.000256	-0.000256	-0.000256

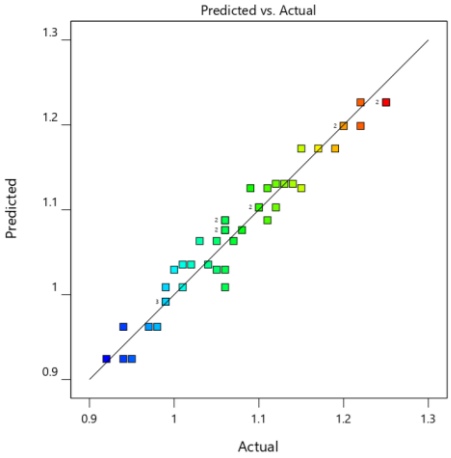

Fig. 7. Model predicted vs. actual data

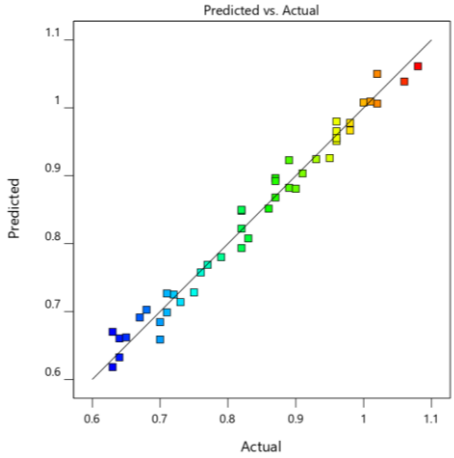

Fig. 8. Model predicted vs. actual data

Table 6. Equation coefficients for the perpendicularity u model

Coefficients	Q1	Q2	Q3	Q4	Q5
α_0	+0.184382	+0.170290	+0.131956	+0.108068	+0.080290
α_1 (p)	-0.000215	-0.000215	-0.000215	-0.000215	-0.000215
α_2 (h)	-0.001936	-0.001936	-0.001936	-0.001936	-0.001936
α_{12} (p×h)	+0.000087	+0.000087	+0.000087	+0.000087	+0.000087

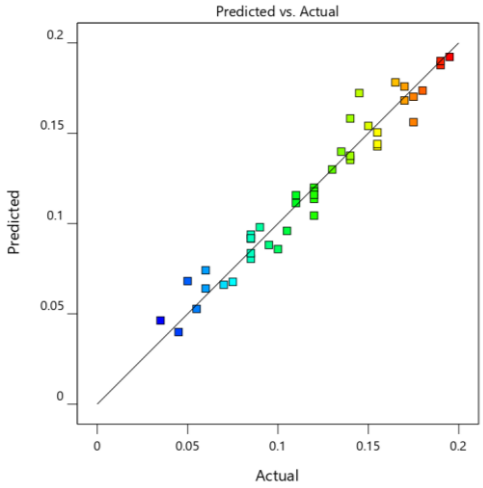

Fig. 9. Model predicted vs. actual data

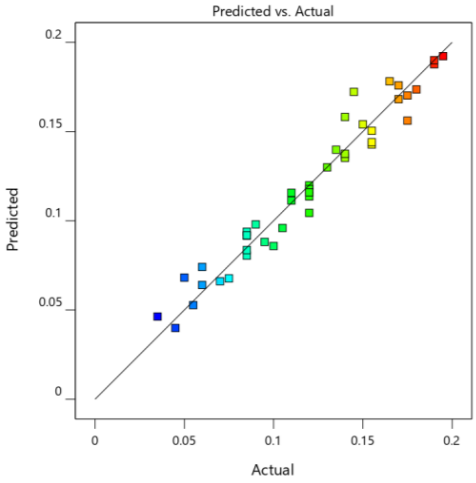

Fig. 10. Model predicted vs. actual data

For the the kerf angle α, the equation coefficients are presented in Table 7. The values predicted by the model closely follow the actual data, as can be seen in Figure 10.

$$\alpha_k(h, p) = \beta_{0k} + \beta_{1k}p + \beta_{2k}h + \beta_{12k}p \times h \quad (8)$$

where $k = 1 \ldots 5$.

Table 7. Equation coefficients for the kerf angle α model

Coefficients	Q1	Q2	Q3	Q4	Q5
α_0	+0.184382	+0.170290	+0.131956	+0.108068	+0.080290
α_1 (p)	-0.000215	-0.000215	-0.000215	-0.000215	-0.000215
α_2 (h)	-0.001936	-0.001936	-0.001936	-0.001936	-0.001936
α_{12} (p×h)	+0.000087	+0.000087	+0.000087	+0.000087	+0.000087

3.3. Process optimization

Process optimization in cases whith multiple outputs can be achieved using desirability functions [13]. In this approach, each response y_i has an associated desirability function d_i with values assigned within the interval [0,1].

As the response y_i gets closer to its goal, the desirability approaches to 1, whereas if the response is getting further away from the goal, the desirability tends to 0. The overall desirability of the model is calculated as

$$D = \left(d_1 d_2 \ldots d_n\right)^{\frac{1}{n}} \tag{5}$$

where n is the number of responses.

For each response the goal can be set as "none", "maximize", "minimize", "target" or "in range". Factors are also included in the optimization and similar goals can be set for them, too.

For the current study, the constraints imposed for the optimization are presented in Table 8. As the objective of the process is to have a good geometry of the cut with the smallest amount of material waste so the goals were set for the minimum width of cut and perpendicularity, and consequently for the kerf angle. As for the input parameters (influence factors), the conditions were as follows. An "in range" condition was set for the cutting quality Q, since is a qualitative factor and it has discrete values. AWJ pressure has a favourable influence on cutting geometry and it also increases process productivity, so the condition was set to maximum value. An "in range" condition was set for the standoff distance.

Table 8. Optimization constraints

Name	Goal	Lower limit	Upper limit
Responses			
Entrance width of cut, Li, [mm]	minimize	0.92	1.25
Exit width of cut, Le, [mm]	is in range	0.63	1.08
Perpendicularity, u, [mm]	minimize	0.035	0.195
Kerf angle, α, [°]	minimize	0.105545	0.588015
Influence factors			
Cutting quality, Q	is in range	Q5	Q1
Pressure, p, [MPa]	maximize	200	300
Standoff distance, h, [mm]	is in range	1	3

The optimum solution had the overall desirability of 0.854, with the following combination of input parameters: cutting quality Q5, AWJ pressure p = 300 MPa, and standoff distance h = 1 mm. The predicted outcomes of this parameters' setup are entrance width of cut Li = 1.063 mm, exit width of cut Le = 0.98 mm, perpendicularity u = 0.04 mm, and kerf angle α = 0.12° (Figure 11). The ramps representations of the optimum solution are presented in Figure 12.

A validation of the results can be done by comparing the model prediction with experimental data as shown in Table 9. There is a good agreement between the two sets of values.

Table 9. Validation of the results

Response	Predicted value	Experimental value	Error %
Entrance width of cut, Li	1.063	1.050	1.22
Exit width of cut, Le	0.98	0.96	2.04
Perpendicularity, u	0.04	0.045	-12.50
Kerf angle, α	0.12	0.1357	-13.08

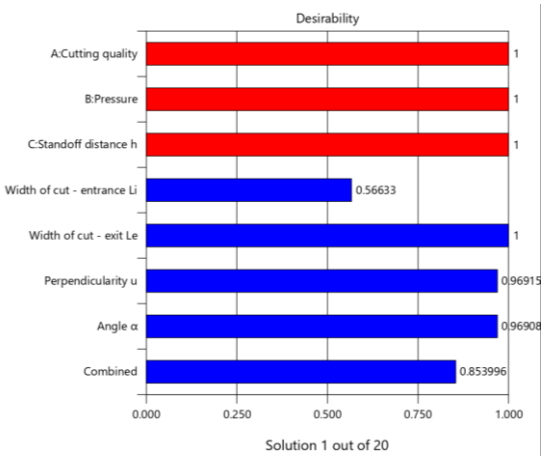

Fig. 11. Desirability bar chart

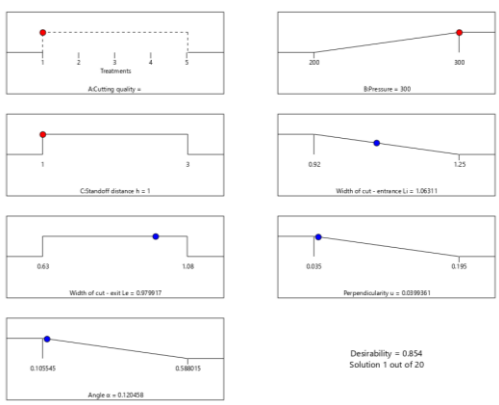

Fig. 12. Ramp functions of the optimum solution

4. CONCLUSIONS

In this work, the RSM approach was applied to study the influence of process parameters on the geometrical parameters of the cut. The most important conclusions coming from the results are formulated below.
ANOVA statistics have revealed that the significant factors are the cutting quality Q and the standoff distance h. Cutting quality Q controls the traverse speed, which reduces from Q1 to Q5. The highest quality, Q5, uses the lowest traverse speed so the errosion rate is higher, which produces larger widths of cut, both at entrance and at exit. At the same time the perpendicularity of the walls improves, meaning that overall, a better cut is produced. When the standoff distance, h, increases the water jet has a wider spread and the geometric parameters of the cut worsens.
Mathematical models of the outputs were formulated, and they offer a very good covering of the experimental space, with PredR^2 values between 0.9228 and 0.9685.
Multiobjective optimisation of the process was performed resulting in an overall desirability of 0.854. Optimal values of the input factors are Q5 for cutting quality, 300 MPa jet pressure, and 1 mm standoff distance. The predicted geometrical parameters of the cut are entrance width of cut Li = 1.063 mm, exit width of cut Le = 0.98 mm, perpendicularity u = 0.04 mm, and kerf angle $\alpha = 0.12°$. The comparison with the experimental result showed a very good agreement.
Further investigations will cover different materials with high applicability to automotive and aerospace industries, various abrasive materials, variable dosage of abrasives, surface qualiy.

REFERENCES

1. Babu, M.N.; Muthukrishnan, N., (2018). *Exploration on Kerf-angle and Surface Roughness in Abrasive Waterjet Machining using Response Surface Method*, J. Inst. Eng. India Ser. C, 99, 645-656.
2. Deshpande, Y.; Brve, P.S.; Mandakar, T.A.; Pund, S.S., (2022). *Optimization of Surface Roughness and Cone Angle in Awj Machining of Aircraft Material Using RSM*, MATTER: Int. J. Sci. Tech., 8 (1), 17-32.
3. Vijayakumar, R.; Srirangarajalu N.; Santhanakumar M.; Edwin Paul N.E.; Rajesh M., (2023). *Investigation of Abrasive Aqua Jet Hole Making (AAJHM) parameters using desirability analysis on Inconel-625 space alloy*, J. Manuf. Proc., 92, 311-328.
4. Sisodia, V.; Gupta, S.K.; Salunkhe, S.; Murali A.P.; Kumar S., (2023). *An Experimental Investigation on Machining of Hardened AISI 440C Stainless Steel Using Abrasive Water Jet Machining Process*, J. of Materi. Eng. and Perform., early access, available online, doi: 10.1007/s11665-023-08040-y.
5. Wang, S.; Hu, D.; Yang, F.; Pin, L., (2022). *Research on Kerf error of aluminum alloy 6061-T6 cut by abrasive water jet*, Int. J. Adv. Manuf. Technol., 118, 2513–2521.
6. Du, M.; Guo, Y.; Wang, H.; Dong, H.; Liang, W.; Wu, H.; Ke, Y., (2023). *Modeling of the cutting front profile in abrasive water jet machining based on the energy balance approach*, Prec. Eng., 79, 210-220.
7. Abushanab, W.S.; Moustafa E.; Harish, M.; Shanmugan, S.; Elsheikh, A., (2022). *Experimental investigation on surface characteristics of Ti6Al4V alloy during abrasive water jet machining process*, Alexandria Eng. J., 61(10), 7529-7539.
8. Llanto, J.M.; Tolouei-Rad, M.; Vafadar, A.; Aamir, M., (2021). *Impacts of Traverse Speed and Material Thickness on Abrasive Waterjet Contour Cutting of Austenitic Stainless Steel AISI 304L*, Appl. Sci., 11, 4925.
9. Joel, C.; Jeyapoovan, T., (2021). *Optimization of machinability parameters in abrasive water jet machining of AA7075 using Grey-Taguchi method*, Mater. Today – Proc., 37, 737-741.
10. Radovanovic, M., (2020). *Multi-Objective Optimization of Abrasive Water Jet Cutting Using MOGA*, Proc. Manuf., 47, 781-787.
11. Ćojbašić, Ž.; Petković, D.; Shamshirband, S.; Tong, C.W.; Ch, S.; Janković, P.; Dučić, N.; Baralić, J., (2016). *Surface roughness prediction by extreme learning machine constructed with abrasive water jet*, Prec. Eng., 43, 86-92.
12. Available from: https://www.omax-france.fr/details-centre+de+decoupe+par+jet+d+eau+abrasif+omax+maxiem+0707+a+toulouse-196.html, Accessed: 24/04/2023 poza masina OMAX
13. Meyers, R.; Montgomery, D.; Anderson-Cook, C., (2009). *Response surface methodology: process and product optimization using designed experiments*, Wiley, New Jersey.

Received: March 12, 2023 / Accepted: December 15, 2023 / Paper available online: December 20, 2023 © International Journal of Modern Manufacturing Technologies